

Development of a new irradiation-embrittlement prediction model for reactor pressure-vessel steels

Qi-Bao Chu¹, Lu Sun², Zhen-Feng Tong², and Qing Wang^{1*}

¹ Nuclear and Radiation Safety Center, Ministry of Ecology and Environment, Beijing, 100082, China

² School of Nuclear Science and Engineering, North China Electric Power University, Beijing 102206, China

Abstract

Predicting the transition-temperature shift (TTS) induced by neutron irradiation in reactor pressure-vessel (RPV) steels is important for the evaluation and extension of nuclear power-plant lifetimes. Current prediction models may fail to properly describe the embrittlement trend curves of Chinese domestic RPV steels with relatively low Cu content. Based on the screened surveillance data of Chinese domestic and similar international RPV steels, we have developed a new fluence-dependent model for predicting the irradiation-embrittlement trend. The fast neutron fluence ($E > 1$ MeV) exhibited the highest correlation coefficient with the measured TTS data; thus, it is a crucial parameter in the prediction model. The chemical composition has little relevance to the TTS residual calculated by the fluence-dependent model. The results show that the newly developed model with a simple power-law functional form of the neutron fluence is suitable for predicting the irradiation-embrittlement trend of Chinese domestic RPVs, regardless of the effect of the chemical composition.

Keywords: Reactor pressure vessel steel, transition temperature shift, irradiation embrittlement, embrittlement trend curve, prediction model

* Corresponding author
Email: wangqingnsc@126.com

1. Introduction

A reactor pressure vessel (RPV) is a key component of a nuclear power plant and serves as a shielding shell to prevent the release of radiation from the reactor core. The replacement of RPVs is unfeasible, considering their high radioactivity and economic efficiency, and their integrity thus determines the safety and lifetime of the reactor [1–6]. According to surveillance programs on the degradation of RPVs, the practical service lifetime of light water reactors (LWRs) is longer than their design lifetime [5]. This suggests that further lifetime extensions to 60 or 80 years could produce significant economic benefits [6]. However, the lifetime extension must be based on an accurate prediction of the irradiation-embrittlement trend of the RPV.

RPVs are usually made of ferrite steel, which has a body-centered cubic structure with minor alloying elements such as Cu, Mn, Ni, and Si; the typical types of RPV steels in LWRs are SA-508III and 16MND5 [7–9]. During reactor operation, the mechanical degradation of RPV steels, which results from neutron irradiation ($E > 1$ MeV), is the main threat to the integrity of the RPV [10–16]. With an increase in the neutron fluence, the ductile-to-brittle transition temperature of the RPV steel shifts to a higher temperature, leading to a decrease in the fracture toughness. Such irradiation embrittlement causes a low-stress rupture of the RPV, which directly threatens the safe operation of the reactor. Therefore, it is necessary to monitor and predict the irradiation-embrittlement trends of RPVs to prevent abrupt failures.

Surveillance programs have been used to evaluate the mechanical performance of RPVs under service conditions in reactors [17]. According to the surveillance programs, the irradiation temperatures and neutron fluences that RPV steels can withstand can be directly derived. Charpy V-notch tests were performed to measure the transition-temperature shift (TTS) of specimens irradiated in a capsule located in the RPV. Based on the measured TTS, particularly the TTS of the Charpy impact energy at 41 J (ΔT_{41J}), the current embrittlement level of the RPV steels can be obtained. Furthermore, the pressure–temperature (P-T) limit curve of the RPV can be adjusted based on the Charpy impact energy results to ensure its safe operation [18].

Because the regulatory experiments could not evaluate the embrittlement tendency of RPVs, several irradiation-embrittlement prediction models [19–27] have been developed to obtain the embrittlement trend curves (ETC), including US RG1.99 (Rev. 2) [21], ASTM E900-02 (Rev. 2007) [22], NUREG/CR-6551 [23], French RCC-M ZG3430 [24], Japanese JEAC4201 [25, 26], *etc.* These models plot the transition-temperature shift (ΔT_{NDT}) as a

function of the neutron fluence (unit: n/cm^2 , $E > 1 \text{ MeV}$) and chemical composition of RPV steels; thus, they can describe the TTS induced by neutron irradiation. Some existing models (for example, US RG1.99 Rev. 2 and French RCC-M ZG3430) were established based on actual RPV surveillance data from their own countries. In other words, the empirical relationship among ΔRT_{NDT} , the neutron fluence, and the chemical composition was derived by fitting the measured TTS data.

Other models, such as US RG1.99 (Rev. 3) [27], ASTM E900-02, and NUREG/CR-6551, further considered the irradiation-embrittlement mechanism of RPV steels when fitting the data. These physics-based models considered the effects of intrinsic defects and Cu/Ni/Mn/Si precipitates on the irradiation embrittlement [28–30], thereby increasing the prediction accuracy. The chemical compositions of RPV steels were demonstrated to be key factors in the available embrittlement prediction models, in which the Cu content had a dominant influence on the ΔRT_{NDT} values. This is because the precipitates in RPV steels are mainly Cu rich, which hinders the dislocation motion and leads to the embrittlement of the materials.

Moreover, RPV steels in international reactors have high Cu content. As a result, the application of these embrittlement prediction models is limited to RPV steels with chemical compositions very similar to those of the corresponding US, French, and Japanese RPV types. For other types of RPV steels, such as Chinese RPV steels with a relatively low Cu content, the current models may fail to obtain an accurate ETC. Recently, machine-learning (ML) models have been employed to predict the ETCs of RPV steels [31–34]. However, the reliability of embrittlement predictions using ML models relies largely on the employed algorithm and training database. Whether an ML model can successfully predict the ETC at neutron fluence ranges beyond the database depends on the extrapolation ability of the algorithm. Therefore, it is necessary to develop a new embrittlement prediction model suitable for Chinese domestic RPV steels with explicit application conditions.

In the present study, we collected surveillance data on international and Chinese domestic RPV steels, including fast neutron fluences, chemical compositions, and measured transition-temperature shifts. Then, using the main chemical composition of Chinese domestic RPV steels as the criteria, the embrittlement data were filtered and divided into training and test sets to fit the new embrittlement prediction model.

Furthermore, we established different functions using the neutron fluences and RPV chemical compositions as the main variables to fit the collected TTS data. By comparing the standard deviations obtained by these functions, we discuss the effects of different features on the fitting quality of the models. As a result, two unified models, i.e., a fluence-dependent model

and a fluence-and-chemical-dependent model, were developed for predicting the irradiation-embrittlement trend for Chinese domestic RPV steels. The prediction accuracy of the two models was then assessed by performing a deviation-band analysis and comparing them with current foreign empirical models. Finally, we employed the new fluence-dependent model to estimate the irradiation-embrittlement trend of a Chinese 300-MW nuclear power plant.

2. Irradiation-embrittlement data

2.1 Data collection

We first collected the available irradiation-embrittlement data for Chinese domestic and international RPV steels (e.g., the US, France, Germany, Japan, Korea, *etc.*). The data included the neutron fluence (unit: n/cm^2 , $E > 1 \text{ MeV}$), transition-temperature shift, $\Delta\text{RT}_{\text{NDT}}$, and chemical compositions of base and weld metals. There are 53 and 144 groups of valid Chinese and international RPV steel embrittlement data, respectively.

The main chemical compositions (Cu, Ni, and P) of the collected international RPV materials are summarized in Fig. 1. The Cu contents of these international RPV steels are mainly in the range of 0.02–0.20 wt.%. Most RPV materials have a relatively high Ni content (0.05–0.09 wt.%) and low P content (0.005–0.015 wt.%). In addition to the chemical composition, the neutron fluence directly affects the transition-temperature shift. These embrittlement data have similar fast neutron ($E > 1 \text{ MeV}$) fluence ranges, which are 1.8×10^{17} – $6.4 \times 10^{19} \text{ n/cm}^2$ for the collected Chinese RPV data and 3.2×10^{18} – $7.4 \times 10^{19} \text{ n/cm}^2$ for the international RPV surveillance data.

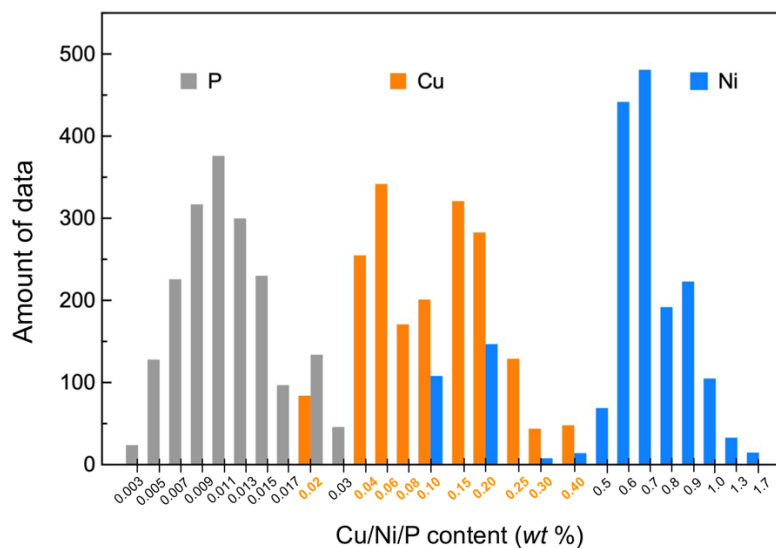


Fig. 1. Ranges of the Cu, Ni, and P content of the collected international RPV materials. The Y-axis represents the amount of data corresponding to a certain range of Cu/Ni/P content listed in the X-axis.

2.2 Data screening

To develop a prediction model suitable for Chinese domestic RPV steels and those with similar chemical compositions, we filtered the collected international RPV embrittlement data, using the chemical compositions (mainly Cu, Ni, P, and Mn) of Chinese domestic RPV steels as the criteria. Consequently, 285 groups of international embrittlement data for RPV base metals were selected as the database to fit our prediction model. The RPV material types in these data were mainly 16MND5, SA508-3, 20MnMoNi55 forging, and SA533-B1 plate. Considering the design standards of Chinese RPV materials, the data for the 20MnMoNi55 and SA533-B1 steels were excluded.

Finally, 126 groups of embrittlement data for international RPV base metals were retained and divided into training (99) and test (27) sets. Similarly, we screened out 46 groups of data for international RPV weld metals as the training set and 44 groups as the test set. The training dataset was used for model fitting and the test dataset was used to assess the fit quality of the developed model.

In addition to international RPV embrittlement data, we screened out 69 and 53 groups of ΔRT_{NDT} data for Chinese domestic RPV base and weld metals, respectively. The average contents of the main chemical compositions (Cu, Ni, Mn, P, Si, and C) of the screened international and Chinese RPV steels are listed in Tables 1 and 2. It can be seen that the chemical compositions of the screened international RPV steels are very similar to those of Chinese RPV data. The only difference is that Chinese RPV steels have a much lower Cu content. Nevertheless, it is reliable to employ international RPV embrittlement data to fit the new prediction model for Chinese domestic RPV steels.

Table 1. Chemical compositions of screened international and Chinese RPV base metals (unit: wt.%)

	Cu	Ni	Mn	P
International SA508-3	0.0403	0.7594	1.3554	0.0066
International 16MND5	0.0621	0.7096	1.3380	0.0070
Chinese RPV	0.0291	0.7340	1.3801	0.0048

Table 2. Chemical compositions of screened international and Chinese RPV weld metals (unit: wt.%)

	Cu	Ni	Mn	P	Si	C
International RPV	0.0325	0.6174	1.5928	0.0082	0.3592	0.0636
Chinese RPV	0.0306	0.7474	1.5245	0.0071	0.3116	0.0762

2.3 Data selection

The testing method and definition of neutron fluence and ΔRT_{NDT} differ for different nuclear power plants. The neutron fluence used as a parameter in the ETC is usually the average of the measured neutron-fluence values. Some Chinese domestic power plants amend the neutron fluences of different base-metal or weld-metal samples, which have different locations in the irradiation surveillance capsule. The amended neutron fluence values are then used to calculate the predictive value of ΔRT_{NDT} . Generally, the base- and weld-metal samples are located on the positive and negative sides of the irradiation surveillance capsule, respectively. The amended neutron-fluence values are typically no greater than 20%.

To evaluate the effects of neutron fluence values on the formula of the developed prediction model, we modified the neutron fluence. In other words, the neutron fluence of the base metal was multiplied by a coefficient of 1.2 and the neutron fluence of the weld metal was multiplied by a coefficient of 0.8. The ΔRT_{NDT} values were refitted using the modified neutron fluences as input parameters. The difference in the calculated ΔRT_{NDT} values was less than 0.23 °C when using the modified neutron fluences as variables in the model. Therefore, considering the measurement uncertainty, the amendment of the different measured neutron fluences can be disregarded in the fitting process of the prediction model.

The ΔRT_{NDT} values are obtained from Charpy impact experiments, which correspond to the temperature change at certain Charpy impact energies or lateral expansions. The determination of the ΔRT_{NDT} values is different for different standard regulations. In the Chinese RPV surveillance program, one way to determine ΔRT_{NDT} is to choose the larger value between the temperature shifts corresponding to the impact energy of 56 J (ΔT_{56J}) and the lateral expansion of 0.89 mm ($\Delta T_{0.89mm}$). Another method is to consider the transition-temperature shift at the Charpy impact energy of 41 J (ΔT_{41J}) as ΔRT_{NDT} , following the ASTM E185 standard regulation.

Some foreign nuclear power plants have also adopted larger TTS values between ΔT_{68J} and $\Delta T_{0.9mm}$ as ΔRT_{NDT} . Based on the experimental data, we collected 121 groups of irradiation surveillance data from Chinese pressurized water reactors (PWRs) and calculated the corresponding TTS values, i.e., ΔT_{41J} , ΔT_{56J} , and $\Delta T_{0.89mm}$, based on the experimental data. According to the results, the ΔT_{56J} and ΔT_{41J} values have a linear relationship, as follows:

$$\Delta T_{56J} = 0.98 \times \Delta T_{41J}. \quad (1)$$

The residual between ΔT_{41J} and ΔT_{56J} shows a normal distribution between -7 °C and 9 °C and the average value lies in the range of -0.6–6 °C. This indicates that the ΔT_{41J} and ΔT_{56J} values can be treated as the same.

We also examined the average difference between ΔT_{41J} and ΔT_{56J} ($\Delta T_{41J} - \Delta T_{56J}$) as a function of the neutron fluence, which varies by only 1 °C, and the correlation coefficient between ($\Delta T_{41J} - \Delta T_{56J}$) and the neutron fluence is 0.046, which is far smaller than 1. This suggests that ΔT_{41J} and ΔT_{56J} have almost the same relationship with the neutron fluence.

Similarly, we fitted the relationship between ΔT_{41J} and $\Delta T_{0.89mm}$, which is also linearly dependent as shown in the following equation:

$$T_{0.89mm} = 0.904 \times T_{41J} + 7.305. \quad (2)$$

The mean value of $\Delta T_{0.89mm}$ is slightly higher than that of ΔT_{41J} . If ΔRT_{NDT} is calculated as the maximum value between ΔT_{41J} and $\Delta T_{0.89mm}$, it is only 2.93 °C higher than the ΔT_{41J} value. According to the above discussion, there were no significant differences in the three values of ΔT_{41J} , ΔT_{56J} , and $\Delta T_{0.89mm}$. Therefore, we employed the measured ΔT_{41J} as ΔRT_{NDT} to fit the embrittlement prediction model.

3. Embrittlement prediction model

3.1. Model development

The transition-temperature shifts were demonstrated to be related to features such as the neutron fluence, neutron fluence rate, temperature, and RPV chemical composition. These parameters contribute differently to the transition-temperature shifts.

To obtain an appropriate weight for each parameter in the embrittlement prediction model, we first calculated the correlation coefficients of these parameters using the measured ΔRT_{NDT} data. The correlation coefficient is calculated based on the covariance and the standard deviation between the variables, which is defined as $\rho_{x,y} = \frac{cov(x,y)}{\sigma_x \sigma_y}$, where $cov(x, y)$ is the covariance between variable x (e.g., neutron fluence) and variable y (e.g., ΔRT_{NDT}). σ_x and σ_y are the calculated standard deviations of variables x and y , respectively.

The calculated correlation coefficients between the different parameters (neutron fluence, neutron fluence rate, temperature, and chemical composition) and the measured ΔRT_{NDT} are shown in Fig. 2. It can be observed that the fast neutron fluence has the largest correlation coefficient with the measured ΔRT_{NDT} , which is greater than 0.5 for both the RPV base and weld metals. This suggests that the fast neutron fluence will have the greatest effect on the transition-temperature shift compared to the other parameters.

In addition to the fast neutron fluence, the Cu content is a critical factor for ΔRT_{NDT} , with a correlation coefficient larger than 0.3. The other chemical compositions, such as Mn, Si, and P, had a weaker correlation with ΔRT_{NDT} . The neutron fluence rate and temperature also have little influence on the transition-temperature shift according to the analysis of the correlation coefficients. Furthermore, these parameters are not independent of each other. The correlation coefficients between the fast neutron fluence and Cu content were 0.332 and 0.413 for the base and weld metals, respectively, but were still smaller than 0.5. This indicates that overfitting should be avoided when these correlated parameters are incorporated into a single fitting equation.

Because the fast neutron fluence was found to be the only parameter that had a strong correlation (correlation coefficient > 0.5) with ΔRT_{NDT} , we first fitted the measured ΔRT_{NDT} data using the fast neutron fluence as the main variable, and then included the influence of different chemical compositions of RPV steels.

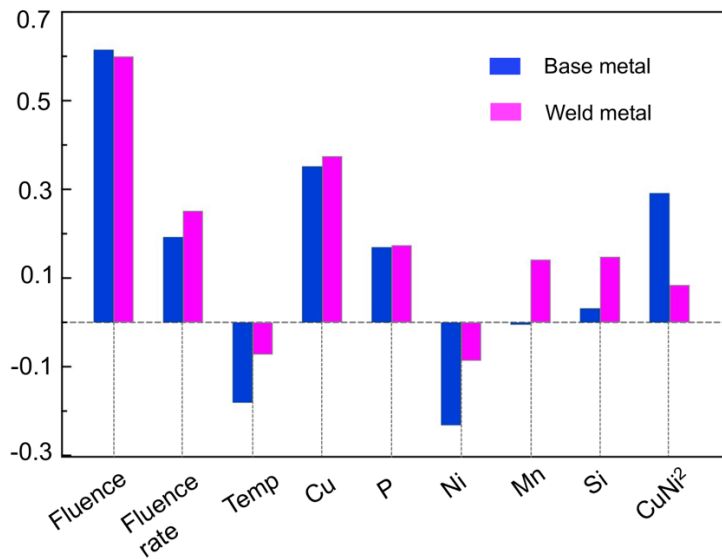


Fig. 2. Correlation coefficients between different parameters with the measured ΔRT_{NDT} data. The blue and magenta bars represent the cases of RPV base and weld metals, respectively.

3.1.1. Fluence dependence

According to current regulatory models and the characteristics of our collected surveillance embrittlement data, the ΔRT_{NDT} values usually show a power-law relationship between the fast neutron fluence (f) and energies larger than 1 MeV. Thus, we employed four power functions to fit the ΔRT_{NDT} data to the neutron fluence; they are defined as fluence-dependent models. The equations for these four functions are as follows:

$$\Delta RT_{NDT} = a \times f^n \quad (3)$$

$$\Delta RT_{NDT} = a \times f + b \quad (4)$$

$$\Delta RT_{NDT} = a \times f^{(b+c \times \log f)} \quad (5)$$

$$\Delta RT_{NDT} = a \times \log_b f + c. \quad (6)$$

Coefficients a , b , and c and power exponent n are all fitted parameters.

Figure 3 shows the predicted trends of ΔRT_{NDT} varying with the fast neutron fluence using the above four equations. The corresponding measured ΔRT_{NDT} data for Chinese and international RPV steels are shown as scatters in Fig. 3 for comparison. Overall, the predicted embrittlement-trend curves (ETCs) cover the measured ΔRT_{NDT} scatters, indicating the reasonable fitting accuracy of these functions. It can be found that the ETCs given by Eq. (6) form the lower bounds for both the base and weld metals, which means that the ΔRT_{NDT} may be underestimated.

The model of Eq. (4) yields the highest overall predicted ΔRT_{NDT} values, indicating an overestimation tendency. The ETCs predicted using Eqs. (3) and (5) are similar and fall into the intermediate region of the four ETCs. These two functions performed better in fitting the measured ΔRT_{NDT} values than Eqs. (4) and (6) did.

We calculated the standard deviation (S_d) obtained from the training ΔRT_{NDT} datasets using the four functions, which were calculated by $\sqrt{s^2} = \sqrt{\frac{\sum_{i=1}^n (x_i - \bar{x})^2}{n-1}}$, where \bar{x} is the mean value of ΔRT_{NDT} and n is the total amount of data. The calculated S_d values are listed in Table 3. Only a small difference appeared between the S_d values of these four functions, which was within 0.5 °C. Notwithstanding, Eqs. (3) and (5) yielded the same S_d values for both the base and weld metals, which were also the lowest among the four models ($S_d = 10.73$ °C for the base metal and $S_d = 11.08$ °C for the weld metal).

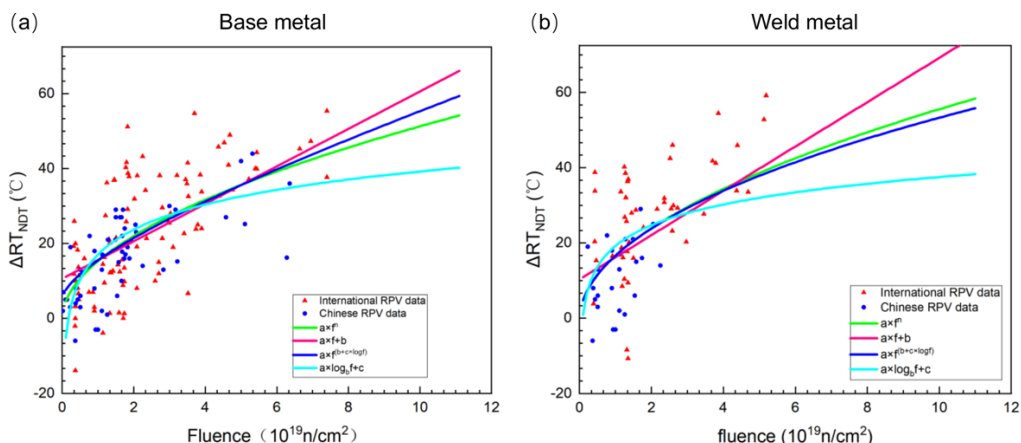


Fig. 3. Embrittlement trend curves predicted by four different functions for (a) the base metal and (b) the weld metal. The measured ΔRT_{NDT} data for Chinese and international RPV steels are denoted by blue circles and red triangles, respectively.

Table 3. Standard deviations (S_d) obtained by the four established fluence-dependent functions

Models	S_d (°C)	
	Base metal	Weld metal
$a \times f^n$ (Eq.3)	10.76	11.13
$a \times f + b$ (Eq.4)	10.79	11.34
$a \times f^{(b+c \times \log f)}$ (Eq.5)	10.73	11.13
$a \times \log_b f + c$ (Eq.6)	11.22	11.69

In the above discussion, the four models were separately fitted for the RPV base and weld metals. In other words, the fitting coefficients of one function are different for the base and weld metals. Therefore, two independent functional relationships were obtained between the RPV base and weld metals. Current embrittlement prediction models, such as the US. RG1.99 (Rev. 2) and French FIS/FIM, adopt the powerful form of Eq. (3) to describe the relationship between the transition-temperature shift and neutron fluence. The fitting results also suggest that Eqs. (3) and (5) yield the lowest standard deviation. In addition, Eq. (3) is simpler than Eq. (5). Therefore, considering the convenience of employing the model to predict ETC in a surveillance program, we chose Eq. (3) to fit the collected ΔRT_{NDT} data and derived the final fluence-dependent embrittlement prediction models for RPV base and weld metals, i.e.,

$$\begin{cases} \Delta RT_{NDT} = 15.311 \times (f \times 10^{-19})^{0.525} & \text{for base metal} \\ \Delta RT_{NDT} = 16.637 \times (f \times 10^{-19})^{0.512} & \text{for weld metal} \end{cases} \quad (7)$$

3.1.2. Chemical-composition dependence

On the basis of the established fluence-dependent embrittlement-prediction model (Eq. 7), the influences of RPV chemical compositions were further included in the model. To obtain appropriate weighting coefficients for each chemical composition, the correlation coefficients between the chemical composition and residual of ΔRT_{NDT} calculated using Eq. (7) were analyzed, as shown in Fig. 4(a). The chemical compositions that have a relatively larger relevance to the ΔRT_{NDT} residual are mainly Cu, Ni, the combined CuNi term, P, Cr, and C. This indicates that these elements may have greater impacts on the fitting results of ΔRT_{NDT} , based on the fluence-dependent model.

The Cr content has the largest correlation coefficient with the ΔRT_{NDT} residual, which is -0.234 for the base metal. The Cu content remains an important factor in the transition-

temperature shift of the RPV base metal, and the correlation coefficients between Cu and CuNi and the ΔRT_{NDT} residual are approximately 0.171 and 0.160, respectively. For the weld metal, the Ni content has the largest correlation coefficient with the ΔRT_{NDT} residual (-0.275), while the P and C content also have small effects on the ΔRT_{NDT} to a certain extent.

Moreover, the relevance of different chemical compositions was analyzed to avoid overfitting. For example, as shown by the correlation matrices in Figs. 5(b) and (c), the chemical compositions strongly interrelate with each other. In particular, the correlation coefficients between P and Cu, P and CuNi, and Mn and Mo are all greater than 0.5. This implies that if one chemical composition is implanted into the model as a parameter, other elements with large correlation coefficients (> 0.5) with this element should be avoided.

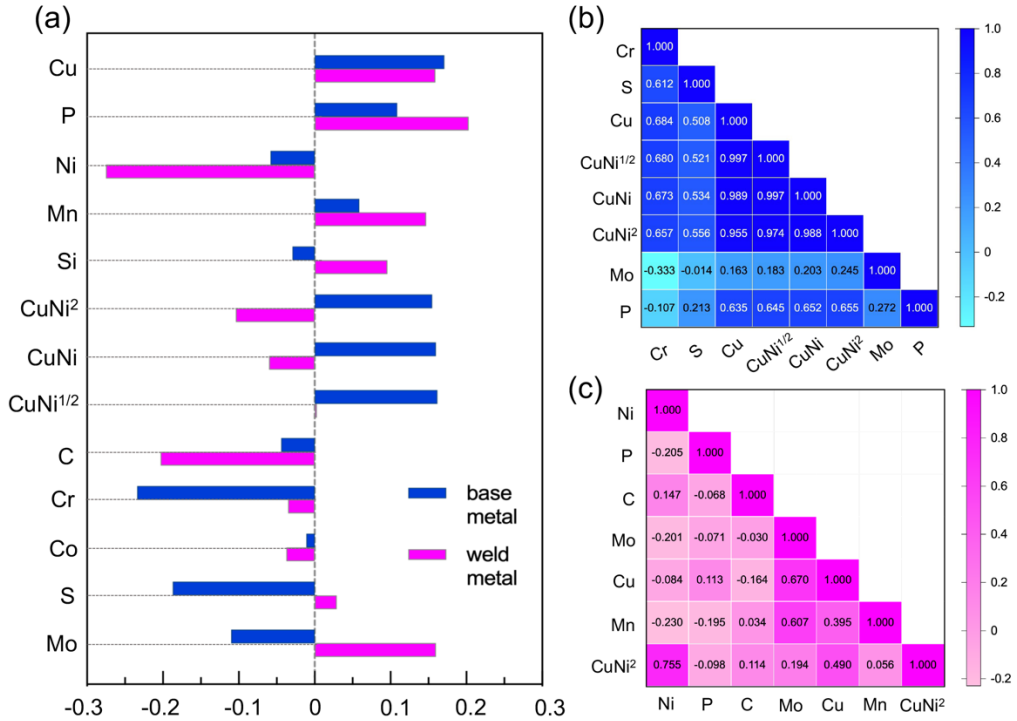


Fig. 4. (a) Correlation coefficients between different chemical compositions and the predicted ΔRT_{NDT} residual. (b) and (c) show the correlation coefficients between different chemical compositions for the RPV base and weld metals, respectively.

We note that the calculated correlation coefficients between different chemical compositions and the ΔRT_{NDT} residual were all lower than 0.3. This means that the RPV chemical compositions may not have a significant effect on the fitting ΔRT_{NDT} values of the fluence-dependent model. On the other hand, most of the collected datasets contained information on Cu, P, Ni, and Mn, but lacked other elements. Therefore, we chose Cu, P, Ni, Mn, and C as the key parameters to conduct the new ΔRT_{NDT} fitting procedure by incorporating both the neutron fluence and different chemical compositions (Cu, P, Ni, Mn, C, and CuNi²)

into one function. Moreover, we constructed different forms of equations with different combinations of RPV chemical compositions, based on the fluence-dependent model.

We found that the changes in the predicted ΔRT_{NDT} values were all less than 1 °C using these equations, regardless of the combination forms of the chemical compositions. Among these functions, Eq. (8) yielded the lowest S_d values for the predicted ΔRT_{NDT} , which were 10.23 °C for the base metal and 10.48 °C for the weld metal.

$$\left\{ \begin{array}{l} \Delta RT_{NDT} = (a + b \times Cu + c \times P + d \times Ni + e \times Mn) \times f^n \text{ for base metal} \\ \Delta RT_{NDT} = (a + b \times Ni + c \times P + d \times C + e \times Cu + g \times Mn) \times f^n \text{ for weld metal} \end{array} \right. \quad (8)$$

It should be noted that the models considering the effects of both the neutron fluence and RPV chemical compositions on the transition-temperature shift have lower standard deviations than the fluence-dependent models (Eq. 7); however, the differences are less than ~0.8 °C. The results suggest that the fluence-dependent model may be sufficiently accurate to predict the ETC of RPV steels.

By contrast, the fluence-and-chemical-dependent model uses RPV chemical compositions as the main parameters; thus, the predicted ΔRT_{NDT} will be disturbed by the RPV material types. Therefore, the fluence-and-chemical-dependent model is limited to certain types of RPV steels that have chemical compositions similar to those in our collected datasets.

3.2. Model assessment

According to the above discussions, we have developed two models, i.e., the fluence-dependent models and the fluence-and-chemical-dependent models (Eq. 7 and Eq. 8, respectively). These models have the same functional forms, but different fitting coefficients for the RPV base and weld metals.

Taking the fluence-dependent models (Eq. 7) as an example, the fitting coefficients are $a = 15.311$ and $n = 0.525$ for the base metal and $a = 16.637$ and $n = 0.512$ for the weld metal. It can be seen that the fitting coefficients for the RPV base and weld metals are very similar to each other, especially the power exponent n of the neutron fluence. Thus, we attempted to use a unified equation to fit the measured ΔRT_{NDT} data for RPV steels without discriminating base and weld metals. The developed unified fluence-and-chemical-dependent prediction model is given as follows:

$$\left\{ \begin{array}{l} \Delta RT_{NDT} = A \times B \times (0.029 + 1.236Cu + 16.932P - 0.555Ni + 0.230Mn) \times (f \times 10^{-19})^{0.504} \\ A = 1.067 \text{ (base metal)}, A = 1.010 \text{ (weld metal)} \\ B = -0.855(T - 292^\circ\text{C}) + 29.238 \end{array} \right. \quad (9)$$

where Cu, P, Ni, and Mn are the mass fractions of the elements. Coefficient A is 1.067 for the base metal and 1.010 for the weld metal, which are almost the same. Coefficient B reflects the

effect of the temperature on the transition-temperature shift, where T represents the inlet temperature of the RPV.

The fluence-dependent model can also have a uniform form for both RPV base and weld metals, which is

$$\left\{ \begin{array}{l} \Delta RT_{NDT} = A \times 15.919 \times (f \times 10^{-19})^{0.521} \\ A = 0.967 \text{ (base metal)}, A = 1.037 \text{ (weld metal)} \end{array} \right. , \quad (10)$$

where coefficient A is 0.967 for the base metal and 1.037 for the weld metal. The power exponent of the neutron fluence is 0.521 for both the base and weld metals. The S_d values of the predicted ΔRT_{NDT} by the unified fluence-dependent model (Eq. 10) are 10.73 °C for the base metal and 10.48 °C for the weld metal. The S_d values given by the unified fluence-and-chemical-dependent model (Eq. 9) are 10.23 °C for the base metal and 11.08 °C for the weld metal, which are very close to those derived by Eq. 10.

The advantage of the above two models is that they have an explicit scope of application, namely, they can be applied to predict the transition-temperature shift of RPV steels irradiated in neutron-fluence ranges of 1.0×10^{17} – 1.11×10^{20} n/cm² and temperature ranges of 280–296 °C. The fluence-and-chemical-dependent model can be applicable to RPV steels with the main chemical compositions (Cu, P, Ni, and Mn) listed in Table 4.

Table 4. Chemical compositions of RPV steels suitable for application in the new model

	Cu (%)	P (%)	Ni (%)	Mn (%)
Base metal	≤0.08	≤0.01%	0.40~0.85	1.15~1.60
Weld metal	≤0.08	≤0.012	≤0.012	≤2.10

Next, we assessed the fitting quality of these two models by plotting the measured ΔRT_{NDT} as a function of the predicted ΔRT_{NDT} , as shown in Figs. 5 and 6 for the fluence-and-chemical-dependent and fluence-dependent models, respectively. The measured ΔRT_{NDT} values were derived from the screened training dataset, which included Chinese and international RPV embrittlement data. The predicted ΔRT_{NDT} values were calculated using Eqs. (9) and (10), respectively. The differences between the predicted and measured Chinese ΔRT_{NDT} are indicated by the triangles and multiple signs in Figs. 5 and 6, respectively. The differences between the predicted and measured international ΔRT_{NDT} are indicated by the diamonds and circles in Figs. 5 and 6, respectively.

It can be seen that most of the data points fall in the vicinity of the 45° line, which indicates that the predicted ΔRT_{NDT} equals the measured ΔRT_{NDT} . In other words, the predicted ΔRT_{NDT} showed a good overall consistency with the measured ΔRT_{NDT} data. Moreover, the majority of data were distributed within the one-fold standard-deviation boundary, the corresponding confidence of which was 68.3%, and almost all the data are within the 95.4% confidence interval.

The deviation-band analyses suggest that our newly developed model has a high accuracy in predicting the irradiation-embrittlement trend for Chinese and similar international RPV steels. Furthermore, the deviation bands of the fluence-and-chemical-dependent and fluence-dependent models are very similar to each other, demonstrating again that the RPV chemical composition has little influence on predicting the transition-temperature shifts.

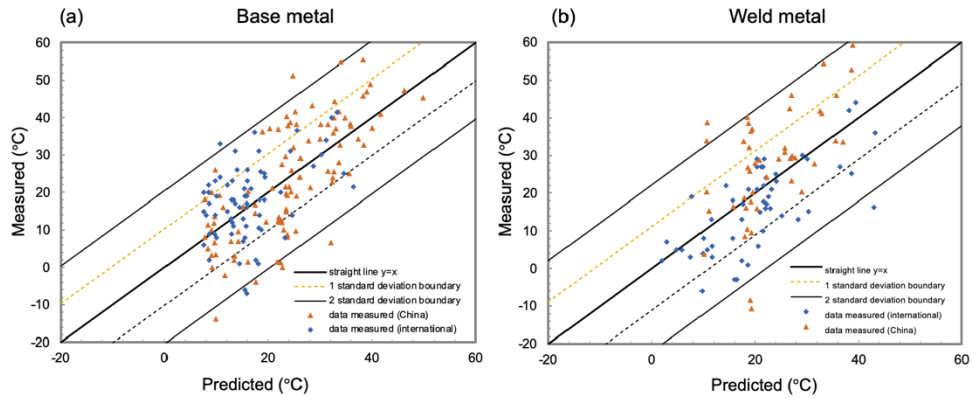


Fig. 5. Distribution of scatterplots of the ΔRT_{NDT} predicted by the fluence-and-chemical-dependent model vs. the measured ΔRT_{NDT} for (a) the RPV base metal and (b) the RPV weld metal.

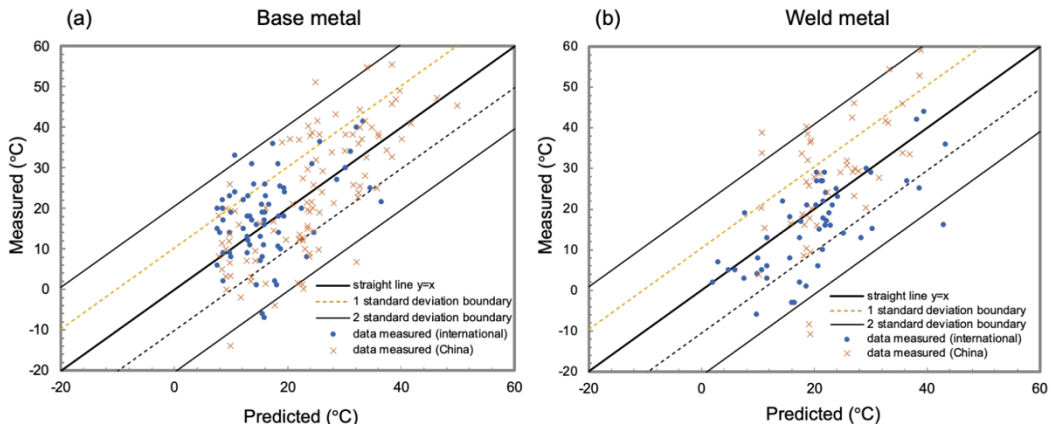


Fig. 6. Distribution of scatterplots of the ΔRT_{NDT} predicted by the fluence-dependent model vs. the measured ΔRT_{NDT} for (a) the RPV base metal and (b) the RPV weld metal.

To evaluate the performance of our developed model compared to current embrittlement-prediction models, such as RG1.99 Rev. 2 and RSE-M2000 and 2010, we employed three

foreign models to calculate the transition-temperature shifts based on our collected ΔRT_{NDT} dataset. The standard deviations obtained using our new models and the other three empirical models are listed in Table 5.

The new fluence-and-chemical-dependent and fluence-dependent models produced the lowest S_d values for both the RPV base and weld metals. This suggests that the newly developed models have higher prediction accuracy than the current US and French prediction models. More importantly, the two new models were suitable for evaluating the embrittlement trends of Chinese domestic RPV steels. We believe that the newly developed fluence-dependent model may have more general application because it avoids the influence of different RPV chemical compositions on the transition-temperature shifts.

Table 5. Standard deviations (unit: $^{\circ}\text{C}$) obtained by different embrittlement prediction models

Models	S_d ($^{\circ}\text{C}$)	
	Base metal	Weld metal
“fluence & chemical dependent” model (Eq.9)	10.23	11.08
“fluence dependent” model (Eq.10)	10.73	10.48
RG1.99 Rev.2	12.07	12.84
RSE-M2000	12.77	12.45
RSE-M2010	11.91	11.80

3.3. Model application

In this section, we employed the established fluence-dependent model to predict the embrittlement trend and the mechanical-property degradation for a Chinese 300-MW nuclear power plant. The embrittlement trend curve estimated by the fluence-dependent model is shown by the red line in Fig. 7; the surveillance data are indicated by black squares for comparison. The available surveillance data fall within the one-fold standard deviation boundary of the calculated ETC. In particular, in the low-flux neutron fluence range ($< 1.0 \times 10^{19} \text{ n/cm}^2$), the estimated ETC is consistent with the measured ΔRT_{NDT} data. Therefore, the newly developed fluence-dependent model can be used to predict the irradiation-embrittlement trend for Chinese RPV steels with reasonable reliability.

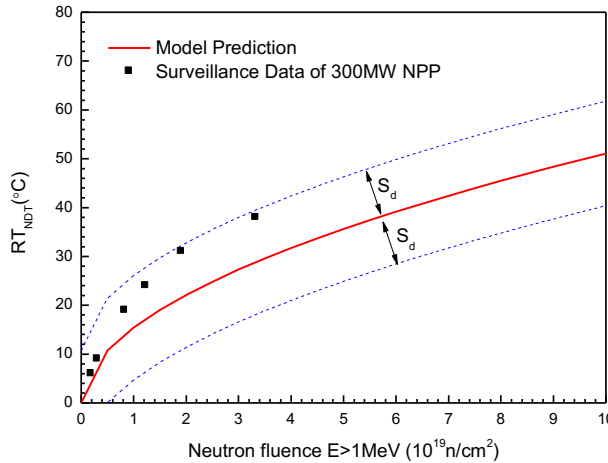


Fig. 7. Embrittlement-trend curve (red line) predicted by the new fluence-dependent model for the Chinese 300-MW nuclear power plant. The black squares represent the surveillance ΔRT_{NDT} data.

In a practical surveillance program, the irradiation-induced degradation of the mechanical properties of RPVs during operation is usually evaluated using two temperature indicators: the adjusted reference temperature (ART) and the pressure–thermal–shock reference temperature (RT_{PTS}). The ART is defined as the sum of the initial RT_{NDT} before irradiation, the irradiation-induced transition-temperature shift ΔRT_{NDT} , and the standard deviations, which are calculated as $2\sqrt{S_{d0}^2 + S_{d\Delta}^2}$. Here, S_{d0} and $S_{d\Delta}$ represent the standard deviations of the measured initial RT_{NDT} and the shifted ΔRT_{NDT} , respectively.

The ART values increase with increasing neutron fluence, indicating that the RPV is at risk of a brittle fracture when its service temperature exceeds the ART. Therefore, according to standard regulation NRC-RG1.99 (Rev. 2), the ART at the one-quarter wall thickness of the RPV cylinder should not be higher than 93°C to avoid a sudden failure. On the other hand, the pressure–thermal–shock temperature will also cause the RPV to fracture; thus, the RT_{PTS} should not exceed 132°C to avoid a sudden RPV failure.

Assuming that the lifetime of RPVs in Chinese nuclear power plants could be extended to 60 years, we calculated the ART at the one-quarter wall thickness of the RPV cylinder and the RT_{PTS} using the newly developed fluence-dependent model to evaluate the embrittlement level of RPVs. The calculation results are listed in Table 6. The calculated ART and RT_{PTS} of RPV steels in the Chinese 300-MW nuclear power plant are 53°C and 62°C , respectively.

In the standard regulation NRC-RG1.99 (Rev. 2), the service temperature limits of RPVs at the end of 60 years of operation are $ART = 93^{\circ}\text{C}$ and $RT_{PTS} = 132^{\circ}\text{C}$. We found that the predicted ART and RT_{PTS} values using the new fluence-dependent model were 40°C and 70°C lower than the temperature limits, respectively. This means that there are still service

temperature margins of 40 °C (ART) and 70 °C (RT_{PTS}) for the safe operation of RPVs prior to a brittle fracture failure. Based on the prediction results, the Chinese 300-MW nuclear power plant has no tendency to fracture within 60 years of operation. Therefore, the design lifetime of the Chinese 300-MW reactor can be extended from 30 to 60 years.

Table 6. Service temperature limits (unit: °C) for the safe operation of an RPV at the end of a 60-year lifecycle

	Predicted	Regulation limit	Margin
ART	53	93	40
RT _{PTS}	62	132	70

4. Conclusions

We developed a new embrittlement-prediction model for RPV steels in Chinese domestic nuclear power plants. The models were fitted based on the collected irradiation-surveillance data of Chinese domestic and international RPV steels, which have similar chemical compositions and are irradiated at similar fast neutron fluence ranges ($E > 1$ MeV).

The newly developed prediction model had a simple form as a power-law function of the fast neutron fluence. The fitting quality of the newly developed fluence-dependent model was only slightly improved when RPV chemical compositions were introduced as the main parameters in the model. The standard deviations given by the newly developed fluence-dependent model were 10.73 °C and 10.48 °C for RPV base and weld metals, respectively, which were lower than current foreign empirical prediction models.

The analysis results showed that the newly developed fluence-dependent model had relatively high accuracy when predicting the irradiation-embrittlement trend of Chinese domestic RPV steels, which were irradiated to a neutron fluence of 1.0×10^{17} – 1.11×10^{20} n/cm² ($E > 1$ MeV) and temperature of 280–296 °C. Based on the new fluence-dependent model, the adjusted reference temperature and the pressure–thermal–shock reference temperature limits of RPVs in the Chinese 300-MW nuclear power plant at the end of 60 years of operation were 53 °C and 62 °C, indicating that the RPVs will have no tendency to fracture within the 60-year operating period.

Acknowledgments

This work was supported by the National Key R&D Program of China through Grant No. 2019YFB1900901 and the Fundamental Research Funds for the Central Universities through Grant No. 2021MS032.

Author contributions

All authors contributed to the study conception and design. Material preparation, data collection and analysis were performed by Qi-Bao Chu, Qing Wang, and Zhen-Feng Tong. The first draft of the manuscript was written by Lu Sun and all authors commented on previous versions of the manuscript. All authors read and approved the final manuscript.

Data Availability Statement

The data that support the findings of this study are openly available in Science Data Bank at <https://cstr.cn/31253.11.sciedb.j00186.00304>, and <https://doi.org/10.57760/sciedb.j00186.00304>.

References

- [1] G.R. Odette, G.E. Lucas, Embrittlement of nuclear reactor pressure vessels. *JOM* **53**, 18-22 (2001). doi:10.1007/s11837-001-0081-0.
- [2] S.J. Zinkle, G.S. Was, Materials challenges in nuclear energy. *Acta Mater.* **61**, 735-758 (2013). doi: 10.1016/j.actamat.2012.11.004.
- [3] J.X. Zuo, W. Song, J.R. An et al., Analysis of heat transfer of the RPV lower head under severe accidents with ASTEC. *Nucl. Tech.* **46**, 010603 (2023). doi: 10.11889/j.0253-3219.2023.hjs.46.010603.
- [4] R.Z. Zhai, B. Zhang, H. Yang et al., Development of a large-deformation model for the pressure-vessel lower head and analysis of its application in the FOREVER experiment. *Nucl. Tech.* **46**, 110606 (2023). doi: 10.11889/j.0253-3219.2023.hjs.46.110606.
- [5] B. Timofeev, Assessment of the first generation RPV state after designed lifetime. *Int. J. Pres. Ves. Pip.* **81**, 703 (2004). doi: 10.1016/j.ijpvp.2004.02.010.
- [6] J.C. van Duysen, G.M. de Bellefon, 60th Anniversary of electricity production from light water reactors: Historical review of the contribution of materials science to the safety of the pressure vessel. *J. Nucl. Mater.* **484**, 209-227 (2017). doi: 10.1016/j.jnucmat.2016.11.013.

[7] Q. Xiong, H.J. Li, Z.P. Lu et al., Characterization of microstructure of A508III/309L/308L weld and oxide films formed in deaerated high-temperature water. *J. Nucl. Mater.* **498**, 227–240 (2018). doi: 10.1016/j.jnucmat.2017.10.030.

[8] X. Dai, B. Yang, The effect of microstructure evolution on fatigue property of SA508Gr.4N steel for nuclear reactor pressure vessels. *J. Nucl. Mater.* **584**, 154544 (2023). doi: 10.1016/j.jnucmat.2023.154544.

[9] X.K. He, C.S. Xie, L.J. Xiao et al., Microstructure and impact toughness of 16MND5 reactor pressure vessel steel manufactured by electrical additive manufacturing. *J. Iron Steel Res. Int.* **27**, 992-1004 (2020). doi: 10.1007/s42243-020-00467-0.

[10] C.W. Li, L.Z. Han, X.M. Luo et al., Effect of tempering temperature on the microstructure and mechanical properties of a reactor pressure vessel steel. *J. Nucl. Mater.* **477**, 246-256 (2016). doi: 10.1016/j.jnucmat.2016.05.017.

[11] R.S. Wang, C.L. Xu, X.B. Liu et al., Microstructural and mechanical studies of reactor pressure vessel steel under proton irradiation. *J. Alloys Compd.* **581**, 788-792 (2013). doi: 10.1016/j.jallcom.2013.07.149.

[12] L.J. Zhou, J. Dai, Y. Li et al., Research progress of steels for nuclear reactor pressure vessels. *Materials* **15**, 8761 (2022). doi: 10.3390/ma15248761.

[13] A. Kryukov, G. Sevikyan, V. Petrosyan et al., Irradiation embrittlement assessment and prediction of Armenian NPP reactor pressure vessel steels. *Nucl. Eng. Des.* **272**, 28-35 (2014). doi: 10.1016/j.nucengdes.2013.12.065.

[14] G.Y. Zhu, C. Guo, Q.F. Liu et al., Numerical simulation on heat transfer of VVER core catcher. *Nucl. Tech.* **46**, 070604 (2023). doi: 10.11889/j.0253-3219.2023.hjs.46.070604.

[15] G.Y. Zhu, J.K. Min, J.P. Jing et al., Numerical simulation on heat transfer in RPV lower head corium pools. *Nucl. Tech.* **45**, 97-102 (2022). doi: 10.11889/j.0253-3219.2022.hjs.45.010605.

[16] H. Yang, B. Zhang, P.C. Gao et al., Development of thermal creep model for reactor pressure vessel lower head and application in OLHF experimental analysis. *Nucl. Tech.* **45**, 080603 (2022). doi: 10.11889/j.0253-3219.2022.hjs.45.080603.

[17] American Society for Testing and Materials International (ASTM) standard E185-16, Standard practice for design of surveillance programs for light-water moderated nuclear power reactor vessels. West Conshohocken, PA. (2015).

[18] T.J. Lee, J.B. Choi, Y.J. Kim et al., A Parametric study on pressure-temperature limit curve using 3-D finite element analyses. *Nucl. Eng. Des.* **214**, 73-81 (2002). doi: 10.1016/S0029-5493(02)00016-X.

[19] G.R. Odette, T. Yamamoto, T.J. Williams et al., On the history and status of reactor pressure vessel steel ductile to brittle transition temperature shift prediction models. *J. Nucl. Mater.* **526**, 151863 (2019). doi: 10.1016/j.jnucmat.2019.151863.

[20] C.L. Li, G.G. Shu, W. Liu et al., The unified model for irradiation embrittlement prediction of reactor pressure vessel. *Ann. Nucl. Energy* **139**, 107246 (2020). doi: 10.1016/j.anucene.2019.107246.

[21] Regulatory Guide, Radiation Embrittlement of Reactor Vessel Materials (Revision 2). Nuclear Regulation Commission, USA (1988).

[22] ASTM E 900-02, Standard Guide for Predicting Radiation-Induced Transition Temperature Shift in Reactor Vessel Materials, ASTM (2007).

[23] E. D. Eason, G. R. Odette, J. E. Wright. Improved embrittlement correlations for reactor pressure vessel steels. NUREG/CR-6551 Nuclear Regulatory Commission, USA (1998).

[24] RCC-M, Design and Construction Rules for Mechanical Components of PWR Nuclear Islands. AFCEN, France (1993).

[25] JEAC 4201, Nuclear Reactor Pressure Vessel Structural Material Surveillance Test Method. JEAC, Japan (1991).

[26] Y. Hashimoto, A. Nomoto, M. Kirk et al., Development of new embrittlement trend curve based on Japanese surveillance and atom probe tomography data. *J. Nucl. Mater.* **553**, 153007 (2021). doi: 10.1016/j.jnucmat.2021.153007.

[27] E.D. Eason, G.R. Odette, R.K. Nanstad et al., A physically-based correlation of irradiation-induced transition temperature shifts for RPV steels. *J. Nucl. Mater.* **433**, 240-254 (2013). doi: 10.1016/j.jnucmat.2012.09.012.

[28] P.B. Wells, T. Yamamoto, B. Miller et al., Evolution of manganese-nickel-silicon-dominated phases in highly irradiated reactor pressure vessel steels. *Acta Mater.* **80**, 205-219 (2014). doi: 10.1016/j.actamat.2014.07.040.

[29] X.Q. Liu, M. Sun, T. Hao et al., Interplay between carbon and substitutional solute atoms during precipitation of Mn/Ni/Si-rich phases in model reactor pressure vessel steels. *Scr. Mater.* **225**, 115158 (2023). doi: 10.1016/j.scriptamat.2022.115158.

[30] Z.Q. Shen, J. Gao, S.S. Lv et al., OKMC simulation of vacancy-enhanced Cu solute segregation affected by temperature/irradiation in the Fe-Cu system. *Nucl. Sci. Tech.* **33**, 149 (2022). doi: 10.1007/s41365-022-01122-x.

[31] Y.C. Liu, H. Wu, T. Mayeshiba et al., Machine learning predictions of irradiation embrittlement in reactor pressure vessel steels. *NPJ Comput. Mater.* **8**, 85 (2022). doi: 10.1038/s41524-022-00760-4.

[32] W.K. He, S.Y. Gong, X. Yang et al., Study on irradiation embrittlement behavior of reactor pressure vessels by machine learning methods. *Ann. Nucl. Energy* **192**, 109965 (2023). doi: 10.1016/j.anucene.2023.109965.

[33] C.L. Xu, X.B. Liu, H.K. Wang et al., A study of predicting irradiation-induced transition temperature shift for RPV steels with XGBoost modeling. *Nucl. Eng. Technol.* **53**, 2610-2615 (2021). doi: 10.1016/j.net.2021.02.015.

[34] J. Mathew, D. Parfitt, K. Wilford et al., Reactor pressure vessel embrittlement: Insights from neural network modelling. *J. Nucl. Mater.* **502**, 311-322 (2018). doi: 10.1016/j.jnucmat.2018.02.027.